AIAA 80-0433R

Comparison of Experimental and Theoretical Turbulence Reduction from Screens, Honeycomb, and Honeycomb-Screen Combinations

James Scheiman* and J.D. Brooks†
NASA Langley Research Center, Hampton, Va.

A ½-scale model of a portion of the NASA Langley 8 ft Transonic Pressure Tunnel was used to conduct some turbulence reduction research. The experimental results are correlated with various theories. Screens alone reduce axial turbulence more than lateral turbulence, whereas honeycomb alone reduces lateral turbulence more than axial turbulence. Because of this difference, the physical mechanism for decreasing turbulence for screens and honeycomb must be completely different. Honeycomb with a downstream screen is an excellent combination for reducing turbulence.

Introduction

In general, the existing turbulence level in the NASA Langley 8 ft Transonic Pressure Tunnel is too high for conducting transition and laminar flow control experiments. Measurements of these turbulence levels are presented in Refs. 1-3. In order to decrease the turbulence levels, the installation of various flow manipulators was proposed. These manipulators would be installed between the last turn and the contraction section.

In order to evaluate the effects of the manipulators, a ½-scale model of a 3 ft^2 stream tube of a section of the tunnel around the fourth corner was constructed as shown in Fig. 1. The manipulators consisted of various combinations of honeycomb and screen mesh. A discussion of the final manipulator configuration selected is presented in Ref. 4. The testing experience directly related to the development of a manipulator configuration for the 8 ft tunnel is presented in Ref. 5 and not considered herein. However, after work on this specific application had been completed, the model became available for conducting some basic research on the performance (turbulence reduction) of various simple one- and two-element manipulator combinations. The performance of such configurations was measured and the data were correlated with available theories. The results of this basic research program are reported herein.

Model and Instrumentation

The ½-scale model used in conducting the tests is shown in Fig. 2. The model consisted of a large bellmouth and transition section (round to square) followed by a nonoperating model of the cooler and the 45 deg turning vanes which simulated the 90 deg turn in the 8 ft tunnel. The cooler consisted of eight rows of closely spaced finned tubes (tubing diameter of about ½ in. and fin diameter of 1⅛ in. with a fin spacing of 14 fins/in.) and caused a pressure drop of about seven times the freestream dynamic pressure. The turn was followed by a long square duct section (18¼ × 18¼ in.) which represented the plenum chamber just upstream of the contraction in the full-scale tunnel. This is the general region where the flow manipulators were installed. The remaining sections of the test model consisted of the instrumentation section, transition and diffuser sections, and the drive section.

The test air speeds in the manipulator and instrumentation sections of the duct were varied between 25 and 60 ft/s. Serious difficulties were encountered with acoustic waves contaminating the hot-wire turbulence measurements. (Hot wires respond to aeroacoustic waves and vorticity turbulence. For a more complete discussion see Ref. 5.) This problem was virtually eliminated by acoustic isolation of the main drive system as shown in Fig. 2. For the tests reported herein a turbulence generator was installed approximately 18 in. downstream of the trailing edge on the centerline of the 45 deg turning vane as shown in Fig. 2. This turbulence generator consisted of a homogeneous porous plate with 3/16 in. diam circular holes that resulted in a 45% open area. For the ½-scale model, the last downstream flow manipulator was approximately 94 in. downstream of the turbulence generator and the hot-wire instrumentation was 12 in. downstream of the last manipulator.

The instrumentation system consisted of acoustic microphones, accelerometers, pitot tubes, pressure transducers, and hot-wire anemometers. Two acoustic microphone systems were used to identify various noise sources, namely by cross correlation and spectra analysis. Noise sources such as the main drive motor, the cooler and/or turning vanes, and excited standing waves could be identified. The accelerometers were used to assure that the hot-wire support system was isolated from various sources of vibration, particularly wall vibrations. The pitot tubes were used to measure the velocities across the test section (velocity survey) and to continually monitor the mean velocity within the duct. (The boundary layer in the duct was found to be about 1 in. thick in the calibrations.) The pressure transducers were used to measure the pressure differences along the duct, across the various manipulators, and for the pitot tube. The hot-wire sensors consisted of both single and crossed wires to measure the axial and lateral turbulence levels. Hot wires were installed both upstream and downstream of the flow manipulators. The upstream hot wires were to assure that the turbulence entering the manipulators was relatively constant for all comparative tests.

The physical properties of the screens and honeycombs used in the investigation are given in Table 1. These devices are indicated throughout this paper by the symbols indicated in the table.

Hot-Wire Measuring Accuracy

In spite of meticulous care, it is difficult to make accurate hot-wire measurements. This problem becomes more difficult when the turbulence levels are very low. However, in order to validate both the turbulence data presented and the conclusions reached, some estimate of accuracy must be attempted.

Presented as Paper 80-0433 at the AIAA 11th Aerodynamic Testing Conference, Colorado Springs, Colo., March 18-20, 1980; submitted March 18, 1980; revision received Sept. 18, 1980. This paper is declared a work of the U.S. Government and therefore is in the public domain.

*Aerospace Engineer, Transonic Aerodynamic Branch, Subsonic-Transonic Aerodynamics Division.
†Aerospace Engineer (retired).

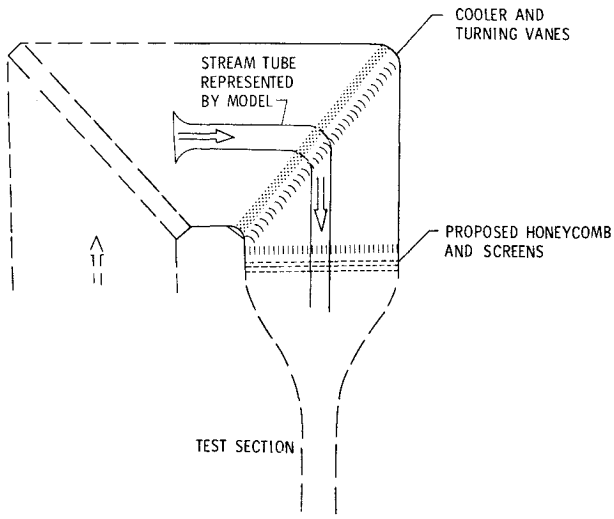

Fig. 1 Section of full-scale tunnel represented by ½-scale model.

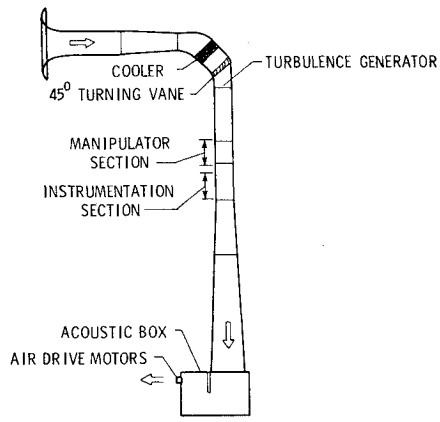

Fig. 2 One-half-scale model used in turbulence reduction program.

Table 1 Physical properties of flow manipulators

Symbol	Mesh, wires/in.	Wire diam, in.	Open area, %
	Screens		
4M	4	0.050	64
8M	8	0.026	63
20M	20	0.009	67
28M	28	0.0075	62
36M	36	0.0065	59
42M	42	0.0055	59
	Honeycomb		
Symbol	Cell size in.	Cell length in.	Gage material in.
1/16M	1/16	0.500	0.001
1/8M	1/8	0.750	0.001
1/4M	1/4	1.50	0.003
3/8M	3/8	3.00	0.003

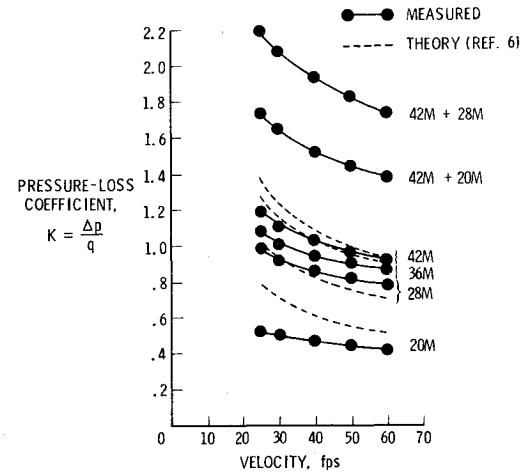

Fig. 3 Pressure-loss coefficient vs duct velocity for various screens and screen combinations.

In an attempt to evaluate the accuracy of the hot-wire data, the data reduction equations were reviewed. This review indicated that an estimate of the accuracy of the measured turbulence due to errors in hot-wire calibration was difficult[5]; therefore, the following procedure was used. Recall that one hot wire (a single wire) was placed between the turbulence generator and the first manipulator. (This wire was used to assure that the turbulence leaving the turbulence generator and/or entering the manipulators was relatively constant.) The measured output from this wire over a 30-day period was tabulated. This tabulation included 175 data points, 5 duct speeds, 2 different hot wires (one was broken during the time period), and many different manipulators. The repeatability of the data was evaluated statistically, that is, the mean and standard deviation, for each of five duct speeds. At a duct speed of 60 ft/s, 95% of the data (2σ point, σ being the standard deviation) fell within ±12% of the mean; at 50 ft/s, the scatter was within ±5.7%; at 40 ft/s, ±4.5%; at 30 ft/s, ±5.7%; and at 25 ft/s, ±5.4%. Since the data obtained at 60 ft/s were quite noisy and had a relatively large scatter, they were disregarded in most of the data presented herein. The standard deviation of the mean value of measured turbulence varies inversely as the square root of the number of data points averaged (i.e., $\sigma_{\bar{x}} = \sigma_x/\sqrt{n}$). In other words, the larger the number of values averaged, the more accurate is the averaged number (mean value). By averaging the turbulence measurements for four speeds (50, 40, 30, and 25 ft/s), the error in the mean value decreases by one-half (i.e., $= 1/\sqrt{4}$). Assuming that the previously estimated errors for one hot wire apply to each of the other wires in the system and averaging the turbulence measurements for one manipulator over the four speeds result in an estimated single-wire accuracy of 2.5-3%.

It is concluded that the axial turbulence measured data presented are accurate to approximately 3%. Examination of the data reduction equations indicated that lateral turbulence measurements would have about twice the error of axial turbulence measurements; hence, it is estimated that the lateral turbulence may have an error as high as 6%.

Discussion of Results

The results presented are actually a small portion of the total amount of data accumulated during the test program. The results are presented in four sections: screens, honeycomb and honeycomb-screen combinations, discussion of theories, and general comments.

Screens

The turbulence reduction theories analyzed herein are based on the screen pressure-loss coefficient K, the pressure-loss coefficient being defined as the pressure loss across the screen Δp divided by the dynamic pressure q of the mean flow through the screen. The theories and some of the physical basis for them are described subsequently in the section on theories.

Figure 3 presents a plot of the measured pressure-loss coefficient vs the duct velocity for various combinations of screens. Reference 6 indicates that for the lower Reynolds

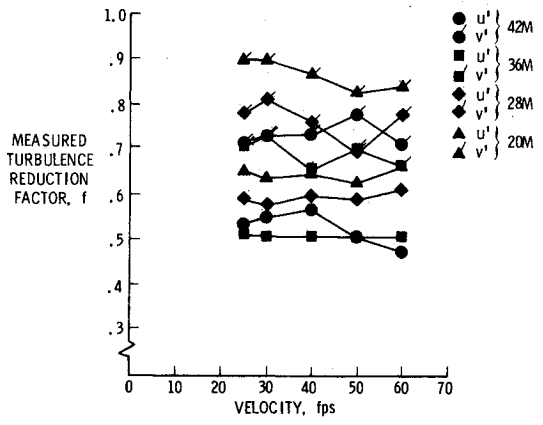

Fig. 4 Measured turbulence reduction factors vs velocity for various screens.

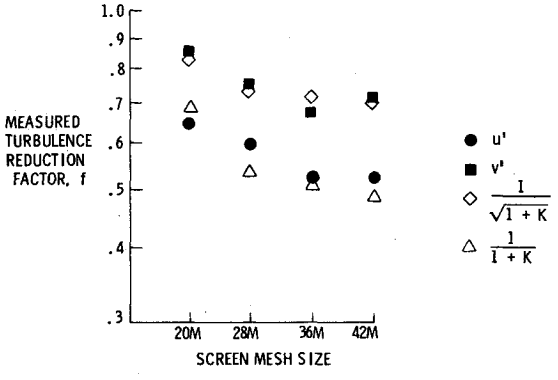

Fig. 5 Turbulence reduction factor for various screens.

numbers the pressure-loss coefficient is equal to

$$K = K_0 + 55.2/R$$

where

$$K_0 = \left(\frac{1-0.95\beta}{0.95\beta}\right)^2$$

$$\beta = \frac{\text{Projected open area}}{\text{Total area}}$$

R = Reynolds number based on wire diameter

(For the tests conducted herein the Reynolds number based on wire diameter varied approximately from 70 to 300.) The corresponding calculated values (from Ref. 6) are shown as dashed lines in Fig. 3 for the single-screen configurations. The agreement with the measured results is not good, qualitative errors in the calculated results being as great as 50%, but the calculated values do show the correct trends with velocity and screen physical characteristics.

The measured data in Fig. 3 indicate that the screen pressure drop, or drag, is not directly proportional to the dynamic pressure. In fact, a curve fit through the experimental data indicates that the pressure drop across the screens varies closely as the velocity varies to the 1.7 power. This pressure drop velocity relationship might have been expected because of the low Reynolds number.

Figure 4 presents a plot of the measured turbulence reduction factor vs velocity. Results are presented for the axial turbulence u' and the lateral turbulence v' for several different single screens, u' and v' being the rms velocity perturbations along the respective axes. The background turbulence measured without manipulators is presented in Table 2. The turbulence reduction factor f was obtained by dividing the turbulence with the manipulators installed by the turbulence without any manipulators. The principal point being illustrated with Fig. 4 is that there is considerable scatter in the data, probably because of measurement inaccuracies, but the data do not indicate any variation of turbulence reduction factor with velocity for any of the screens. Analysis throughout the remainder of this paper based on values of the turbulence reduction factor averaged over the speed range can therefore be expected to present a reasonably accurate and more easily understood picture of the turbulence reduction effectiveness of the various manipulator configurations. Figure 5 presents a plot of the average turbulence reduction factor f for the four screens of Fig. 4. The plot has measured values for both the u' and v' turbulence reduction and theoretical values predicted by the relation $f = 1/\sqrt{1+K}$ from Refs. 7 and 8 and the relation $f = 1/(1+K)$ from Ref. 9. The screens reduce axial turbulence more than lateral turbulence; also the finer mesh screens (which are also the least porous) give a greater reduction in turbulence. Also the factor $1/(1+K)$ predicts the reduction in axial turbulence fairly well, while the factor $1/\sqrt{1+K}$ predicts the reduction in lateral turbulence. A consequence of the fact that the screens reduced axial turbulence more than lateral turbulence is that, if the turbulence upstream of the screen is isotropic (as it is herein), the turbulence will not be isotropic after passing through the first screen. This would be expected to have important consequences when screens are used in combination with other screens.

Table 2 Turbulence without manipulators

v, ft/s	u', %	v', %
60	2.84	2.96
50	2.64	2.85
40	2.29	2.59
30	2.34	2.55
25	2.33	2.63
Average	2.48	2.72

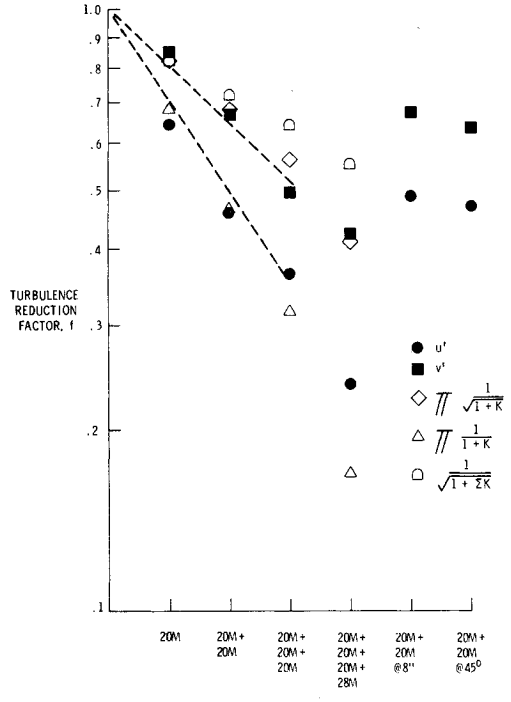

Fig. 6 Turbulence reduction factor for various screen and screen combinations. Note two 20-mesh screens at different screen spacing and two 20-mesh screens with wire weaves at 45 deg to each other.

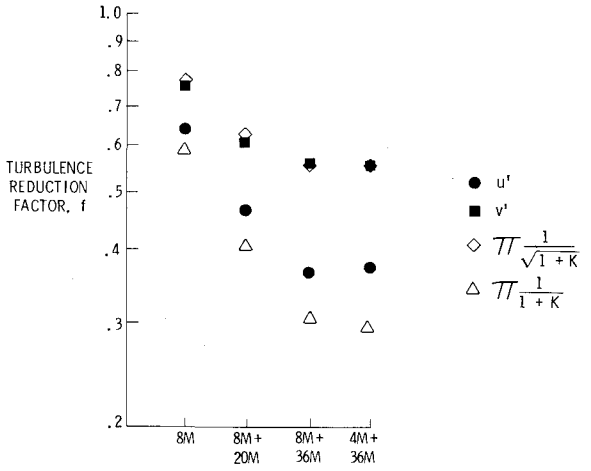

Fig. 7 Turbulence reduction factor for various screens and screen combinations.

Figure 6 presents a plot of the turbulence reduction factor for various combinations of manipulators. The order of the first four screen configurations on the abscissa was selected to indicate the effect of adding screens in series. In Fig. 6, all screens had a 4 in. separation distance, except for one case that will be discussed subsequently. It would seem logical that each screen would reduce the turbulence incoming to it by its turbulence reduction factor f so that the total turbulence reduction factor for a series of screens would be equal to the product of the individual reduction factors, or Πf. The experimental data indicate this to be approximately correct as indicated by the dashed lines fairing the data in Fig. 6. This result is supported by the fact that when the factor $1/\sqrt{1+K}$, which seemed in Fig. 5 to predict the turbulence reduction factor of one screen for lateral turbulence, is applied as $\Pi(1/\sqrt{1+K})$, it predicts the performance of a series of screens on lateral turbulence fairly well. Also, the factor $1/(1+K)$, which seemed to predict the turbulence reduction factor of one screen for axial turbulence, when applied as $\Pi[1/(1+K)]$, predicts the axial performance of a series of screens fairly well. A consequence of the fact that a series of screens gives a turbulence reduction which is equal to the product of their individual turbulence reductions is that one screen which had the same pressure drop as a series of screens would not be as effective. This fact is illustrated by the values of the factor $1/\sqrt{1+\Sigma K}$ in Fig. 7 which indicates less lateral turbulence reduction than the value of the factor $\Pi(1/\sqrt{1+K})$ which accurately predicted the measured turbulence.

The last two cases shown in Fig. 6 (at the extreme right) are for two 20-mesh screens, one with an 8 in. spacing between screens and the other with one screen mesh rotated 45 deg with respect to the other. Both of these cases show an insignificant variation from the case of two 20-mesh screens with a 4 in. spacing.

Figure 7 presents further data to supplement the previous two figures except that a much coarser screen is used as the initial screen. These data show that the coarse 8-mesh screen had about the same effectiveness in reducing turbulence, either alone or in combination with a 20-mesh screen, as the finer 20-mesh screen in Fig. 6, at least for the scale of turbulence of the present experiment. Note also that the calculated turbulence reduction results confirm the previous conclusion that calculations based on the relation $\Pi(1/\sqrt{1+K})$ agree better with the measured values of v' and calculations based on $\Pi[1/(1+K)]$ agree better better with the measured values of u'.

Honeycomb and Honeycomb-Screen Combinations

Figure 8 is a plot of speed vs the measured static pressure loss across the honeycomb used in this test. Unfortunately, the only results measured are for the ¼ in. honeycomb. The honeycomb depths were chosen on the basis of the recommendations in Ref. 10 and unpublished data and vary between six and eight times the cell diameter. Further, H.M. Nagil, one of the authors of Ref. 10, indicated that for honeycomb-screen combinations, the honeycomb should be installed upstream of the screens. This recommendation was followed herein. Figure 8 shows that the pressure loss varies linearly with the velocity rather than velocity squared.

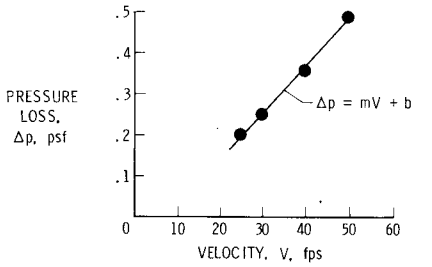

Fig. 8 Measured pressure loss and pressure-loss coefficient vs velocity for ¼ in. honeycomb manipulator.

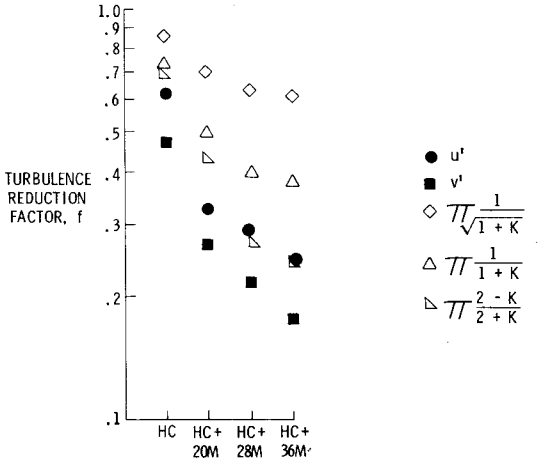

Fig. 9 Turbulence reduction factor for ¼ in. honeycomb alone and in combination with various screen mesh sizes.

Figure 9 presents the measured turbulence reduction factor for the ¼ in. honeycomb alone and in combination with different single screens. Note that, unlike screens alone, honeycomb alone or in combinations with a screen, reduces lateral turbulence more than axial turbulence. A comparison of the turbulence reduction performance of configurations with honeycomb with that of configurations with screens alone is presented in Fig. 10 which was plotted from data of Figs. 6 and 9. Figure 10a shows that configurations with honeycomb were much more effective in reducing lateral turbulence, as would be expected. The comparison in Fig. 10b, however, is surprising in that it shows that the configurations with honeycomb (which is not noted for damping axial turbulence) reduced axial turbulence considerably more than did configurations of screens alone. In fact, the honeycomb with one screen was fully as effective as the configuration of three screens in reducing axial turbulence.

The published theories defining the turbulence reduction for manipulators are very general, as will be discussed later in this paper. While these theories have been primarily correlated with results from screen manipulators, they might also be applied to honeycomb manipulators as was done herein. The pressure-loss coefficient K for the honeycomb is taken as the average value over the speed range.

Figure 9 shows the previously presented theoretical turbulence reduction factors, namely, $(1/\sqrt{1+K})$ (Ref. 7) and $1/(1+K)$ (Ref. 9). Neither of these relations shows reasonable correlation. Therefore, the results of a third theory as presented in Ref. 11 was introduced, namely, $f=(2$

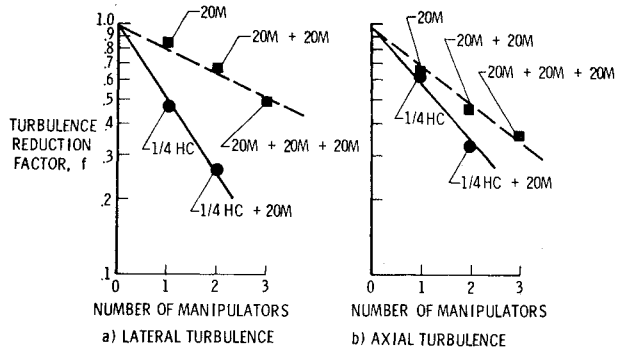

Fig. 10 Comparison of turbulence for configurations with and without honeycomb.

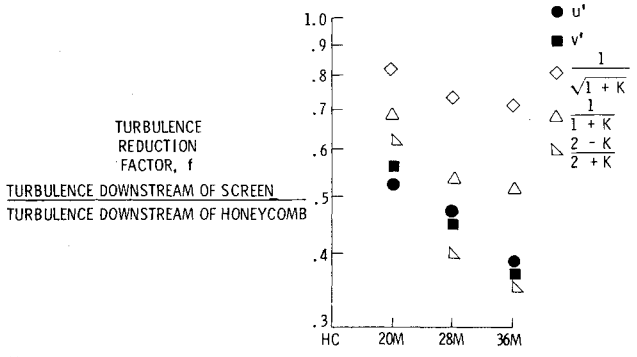

Fig. 11 Turbulence reduction factor for screens downstream of ¼ in. honeycomb.

$-K)/(2+K)$. This theory also did not show reasonable correlation. It was assumed that the lack of correlation of the theories was primarily due to the performance of the honeycomb manipulator; therefore, Fig. 11 was prepared. To obtain the data in Fig. 11, the experimental data in Fig. 9 was rearranged such that turbulence without the manipulator was actually the turbulence downstream of the honeycomb. In other words, the "baseline turbulence" downstream of the honeycomb replaced that of the empty duct. The three theoretical results are also presented. Figure 11 shows that the first two factors $1/\sqrt{1+K}$ and $1/(1+K)$ which had previously shown agreement with lateral and axial turbulence, respectively, greatly underestimate the turbulence reduction factor, whereas the third factor $(2-K)/(2+K)$ yielded a mixture of under- and overestimates. The lack of correlation of the factors $1/\sqrt{1+K}$ and $1/(1+K)$ in this case might be the result of a mechanism described later under General Comments.

Figures 12 and 13 present plots of the turbulence reduction factor for various honeycomb mesh sizes. Figure 12 had a 2 Hz high-pass filter, whereas Fig. 13 had a 100 Hz filter. The u' component of turbulence in Fig. 12 is higher than that in Fig. 13 because of a high-amplitude, low-frequency unfiltered noise source that was not present for the data presented in Fig. 13. The results indicate, as previously noted in connection with the data of Fig. 9, that the v' component of turbulence is lower than that of the u' component, just the opposite of the trend for screens alone. These two figures also indicate there may be an optimum honeycomb mesh size, but the data are not consistent enough to support any conclusion.

Discussion of Theories

In Ref. 7, the mean resistance of the screen to turbulence, or the energy change across the screen KE_2', is equated to the difference between the upstream turbulent energy E_1' and the downstream turbulent energy E_3' or

$$KE_2' = E_1' - E_3'$$

It is reasoned that the turbulence downstream of the screen

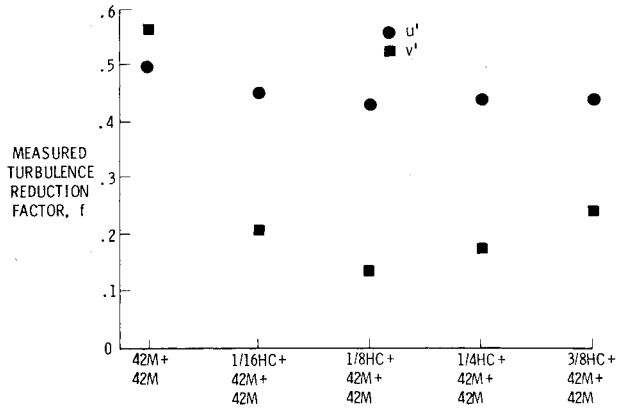

Fig. 12 Turbulence reduction factor for two 42-mesh screens alone and in combination with various upstream honeycomb mesh sizes.

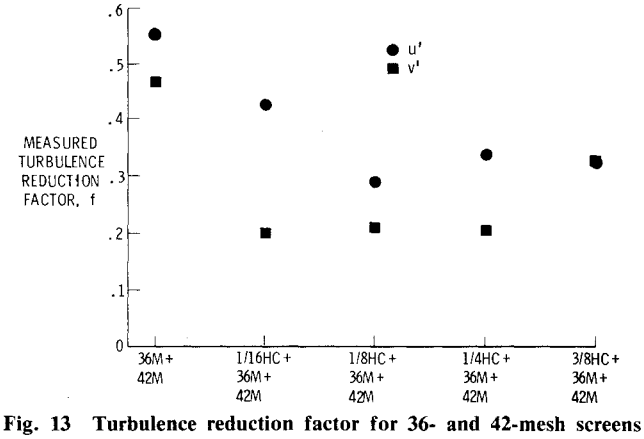

Fig. 13 Turbulence reduction factor for 36- and 42-mesh screens alone and in combination with various upstream honeycomb mesh sizes.

cannot change after it leaves the screen; in other words, change in turbulence due to the screens occurs on the upstream side only, i.e., $E_2' = E_3'$. Since the turbulence velocity is proportional to the square root of the turbulent energy, the turbulent reduction factor becomes $u_3'/u_1' = 1/\sqrt{1+K}$. The experimental data presented in Refs. 7 and 8 seem to verify this theoretical decay law.

In Ref. 9, Prandtl states that screens can be used to obtain a more uniform velocity distribution across the duct section and that a moderate velocity difference is approximately lowered by the factor $1/(1+K)$. This factor has been extended to apply to turbulence reduction across a screen.

In Ref. 11, Collar uses Bernoulli's equation to equate the total pressure loss across the screen to the difference in total pressure upstream and downstream. The axial force across the screen is then equated to the change in axial momentum. Using these two equations and assuming that the turbulent velocities are small compared to the mean velocity, Collar shows that the turbulence reduction for u' becomes equal to $(2-K)/(2+K)$.

In Ref. 12, a more elaborate analysis is presented. Taylor and Batchelor account for the fact that if the flow is nonnormal to the manipulator upstream it will be turned toward the normal downstream. Further, they show from experimental data that for a given screen over nominal velocity range the ratio α of the flow angle normal to the screen downstream ϕ to the flow angle normal to the screen upstream θ is approximately constant. Further, from the test data[8] the ratio $\alpha = 1.1/\sqrt{1+K}$, and this ratio is approximately equal to the lateral turbulence reduction factor. By using potential flow theory and accounting for the boundary conditions on both sides of the screen they show that the axial turbulence reduction factor becomes $(1+\alpha-\alpha K)/(1+\alpha+K)$. By definition of $\alpha = \phi/\theta$, α can vary between 0

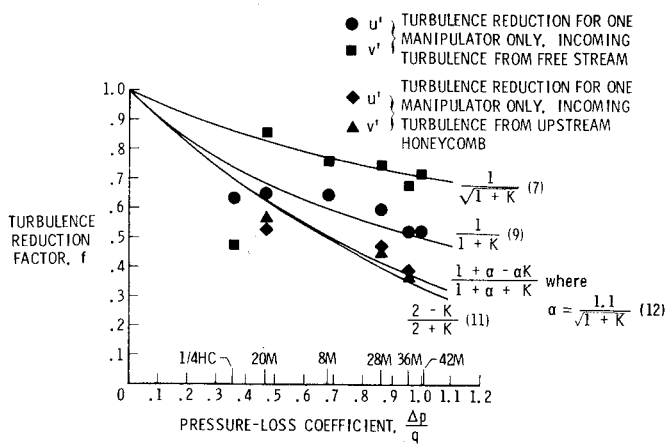

Fig. 14 Measured turbulence reduction factor for various screens and combinations of screens with honeycomb compared with different theories.

and 1. In Ref. 12, Taylor and Batchelor show that when $\alpha = 0$ their axial turbulence reduction is identical with that of Prandtl[9] and when $\alpha = 1$, their reduction factor becomes identical to Collar.[11] The theory in Ref. 12 is the only one that offers a lateral turbulence reduction factor. All these theories assume that the upstream turbulence is isotropic.

The results of the various theories are shown in Fig. 14 where the turbulence reduction factor is plotted against the manipulator pressure-loss coefficient K. Also shown along the abscissa in Fig. 14, are the equivalent K values for various manipulators used in the present study, and experimental data for these manipulators are presented. Considering the screens alone, the axial turbulence reduction appears to agree with Prandtl's relation $f = 1/(1+K)$ and the lateral turbulence seems to agree with Dryden and Schubauer's relation $f = 1/\sqrt{1+K}$. The test data for the honeycomb alone ($K \approx 0.36$) indicates that, unlike the screens, the lateral turbulence is much lower than the axial turbulence and further both experimental reduction factors are appreciably smaller (greater turbulence reduction) than for any of the theories presented.

The data shown for the honeycomb and screen combination are for the screen reduction factor only (i.e., the upstream turbulence for the screens is nonisotropic; in fact, it is the turbulence that is shed downstream of the honeycomb). The correlation with the theories is poor, although it appears that the theory in Ref. 12 provides the best correlation.

General Comments

Because of the differences in reduction factors for screens alone, honeycomb alone, and screens in combination with honeycomb, their mechanism of reducing turbulence must be different. In fact the mechanism for manipulating the turbulence is quite complex and little understood. Because of conservation laws the manipulators basically change the characteristics of the turbulence. In addition, they create their own shed turbulence which is added to the flow stream, the combination of which eventually is absorbed by means of fluid viscosity.

It appears that honeycomb is an excellent absorber of lateral turbulence. It is difficult to imagine how any lateral turbulence (other than that smaller than the honeycomb cell size) can get through the honeycomb; and such small scale turbulence would decay rapidly due to viscosity. On the other hand, it is difficult to imagine that the honeycomb can absorb any axial turbulence directly (since in general the pressure drop is quite small). It could however be visualized as reducing lateral turbulence directly with a subsequent reduction in axial turbulence as a result of the exchange of energy between the axes as the turbulence tends to become isotropic downstream. Such a mechanism might explain the fact brought out in connection with Fig. 10 that the honeycomb reduced axial turbulence as much as a screen while reducing lateral turbulence even more.

Screens behave differently than honeycomb. As the flow angle with respect to the normal to the screen increases as a result of lateral turbulence, the open screen area decreases. However, for low values of turbulence this effect is expected to be small. For axial variations in velocity, the screens will have a tendency to smooth out (spread out) the higher velocity regions into the lower velocity regions and result in a more uniform flow. This arises because of the relatively higher pressure loss across the screen. Therefore, screens will be more effective in reducing axial turbulence than in reducing lateral turbulence.

The data show that screens downstream of honeycomb have a better performance than screens alone. It appears that turbulence downstream of honeycomb is higher in the axial direction than in the lateral direction, and it is axial turbulence that screens are most capable of reducing. Therefore, the combination of honeycomb to reduce the lateral turbulence followed by a screen to reduce the axial turbulence created by the honeycomb provides an excellent combination for reducing overall turbulence.

Conclusion

Tests of screens, honeycomb, and various combinations of these turbulence manipulators have been conducted. The axial and lateral turbulence and pressure loss for these manipulators have been measured. Various theories intended to predict the turbulence reduction have been discussed and correlated with the experimental results. For the same isotropic upstream turbulence, screens reduce axial turbulence more than lateral turbulence. The axial turbulence reduction for screens agrees with Prandtl's theory $1/(1+K)$, whereas the lateral turbulence reduction agrees with Dryden and Schubauer's theory $1/\sqrt{1+K}$. Honeycomb, on the other hand, reduces the lateral turbulence more than the axial turbulence. Because of this difference, the physical mechanism for decreasing turbulence for screens and honeycomb must be completely different, and these mechanisms are speculated on herein. The turbulence reduction of a screen when placed downstream of honeycomb is far better than that for the screen alone, with the result that honeycomb with a downstream screen is an excellent combination for reducing turbulence.

References

[1] Owen, F.K., Stainback, P.C., and Harvey, W.D., "Evaluation of Flow Quality Measurements in Two NASA Transonic Wind Tunnels," AIAA Paper 79-1532, July 23-25, 1979.

[2] Keefe, L.R., "A Study of Acoustic Fluctuations in the Langley 8-Foot Transonic Pressure Tunnel," NASA CR-158983, Jan. 1979.

[3] Brooks, J.D. and Stainback, P.C., "Additional Flow Quality Measurements in the Langley 8-Foot Transonic Pressure Tunnel," AIAA Paper 80-0434, March 18-20, 1980.

[4] McKinney, M. and Scheiman, J., "Evaluation of Turbulence Reduction Devices for the Langley 8-Foot Transonic Pressure Tunnel," NASA TM-81792, June 1981.

[5] Scheiman, J., "Some Considerations of the Configuration and Installation of Honeycomb and Screens to Reduce Wind Tunnel Turbulence," NASA TM-81868, Aug. 1981.

[6] De Vahl, D.G., "The Flow of Air Through Wire Screens," *Hydraulics and Fluid Mechanics,* R. Silvester, ed., Pergamon Press, 1964, pp. 191-212.

[7] Dryden, H.L. and Schubauer, G.B., "The Use of Damping Screens for the Reduction of Wind Tunnel Turbulence," *Journal of Aeronautical Sciences*, Vol. 14, April 1947, pp. 221-228.

[8] Schubauer, G.B., Spangenburg, W.G., and Klebanoff, P.S., "Aerodynamic Characteristics of Damping Screens," NACA TN 2001, Jan. 1950.

[9] Prandtl, L., "Attaining a Steady Air Stream in Wind Tunnels," NACA TM 726, Oct. 1933.

[10] Loehrke, R.I. and Nagib, H.M., "Experiments on Management of Free-Stream Turbulence," AGARD Rept. 598, Sept. 1972.

[11] Collar, A.R., "The Effects of a Gauze on the Velocity Distribution in a Uniform Duct," R&M No. 1867, British A.R.C., Feb. 1939.

[12] Taylor, G.I. and Batchelor, G.K., "The Effect of Wire Gauze on Small Disturbances in a Uniform Stream," *Quarterly Journal of Mechanics and Applied Mathematics,* Vol. II, Pt. 1, March 1949, pp. 1-29.